Science Advances
AAAS

advances.sciencemag.org/cgi/content/full/6/33/eabb7043/DC1

Supplementary Materials for

A durable nanomesh on-skin strain gauge for natural skin motion monitoring with minimum mechanical constraints

Yan Wang, Sunghoon Lee, Tomoyuki Yokota, Haoyang Wang, Zhi Jiang, Jiabin Wang, Mari Koizumi, Takao Someya*

*Corresponding author. Email: someya@ee.t.u-tokyo.ac.jp

Published 12 August 2020, *Sci. Adv.* **6**, eabb7043 (2020)
DOI: 10.1126/sciadv.abb7043

This PDF file includes:

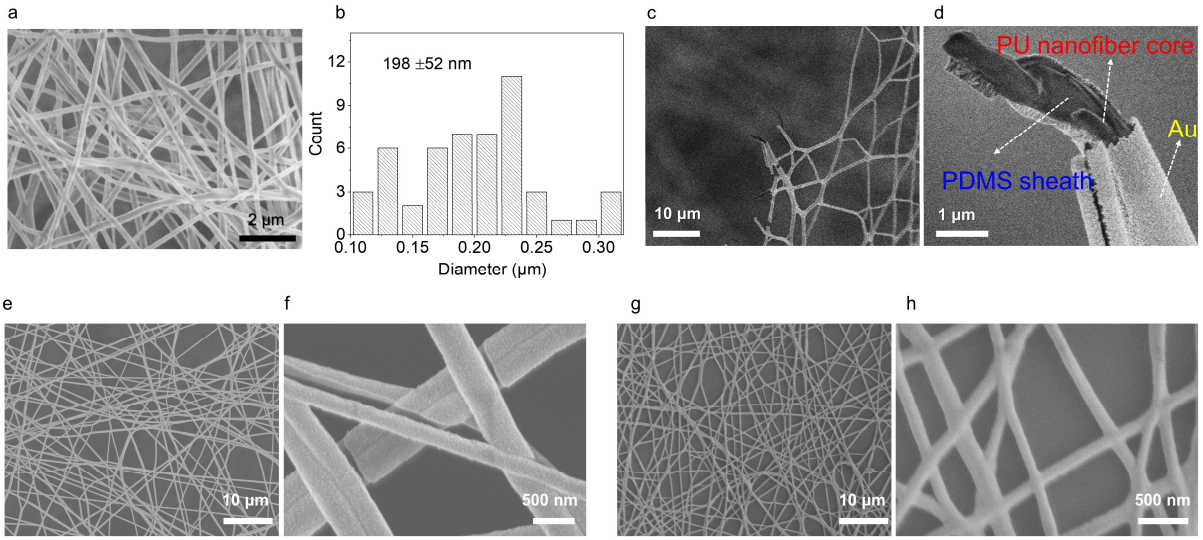

fig. S1. PU nanofiber diameter distribution and SEM characteristics of PU nanofiber, PU–PDMS nanomesh, Au/PU nanomeh, and Au/PU–PDMS nanomesh. **a**. SEM image of PU nanofibers. **b**. Diameter frequency of PU nanofibers. Statistical data on the diameter distribution was done by image processor (image J) on a) SEM image. N=50. **c-d**. SEM images of SEM images of PU–PDMS core-sheath nanomesh configurations. Samples are made by cutting. **e-f**. SEM images of bare PU nanomesh conductor. **g-h**. SEM images of PU–PDMS nanomesh conductor. PDMS/hexane w/w: 1/160.

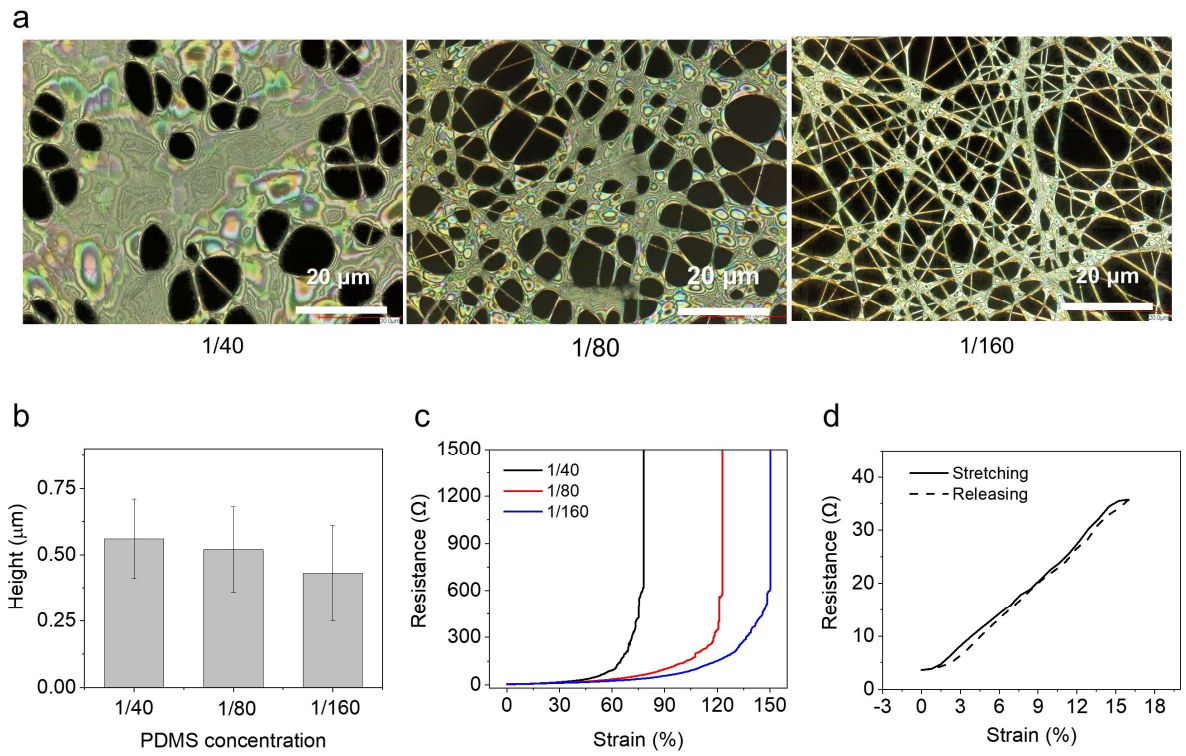

fig. S2. Microscopical images, height, and electromechanical characterizations of different PU–PDMS nanomesh devices. w/w of hexane/PDMS=1/40, 1/80, and 1/160. **a.** Microscopical images of different PU–PDMS nanomeshes. **b.** Height comparison of three different devices. The error bars are obtained by calculating standard deviations from the height profiles. **c.** Electromechanical properties comparison of three different devices. **d.** Hysteresis evaluation. The degree of hysteresis (HD) is defined as $\frac{A_1-A_2}{A_1}\cdot 100\%$, A_1 and A_2 are the areas of stretching and releasing curves, respectively. Resistance (R) is recorded as a function of time while a dynamic strain from 0–16% strain (ε) is subjected to the PU–PDMS nanomesh strain gauge at a frequency of 1 Hz. w/w of hexane/PDMS=1/40.

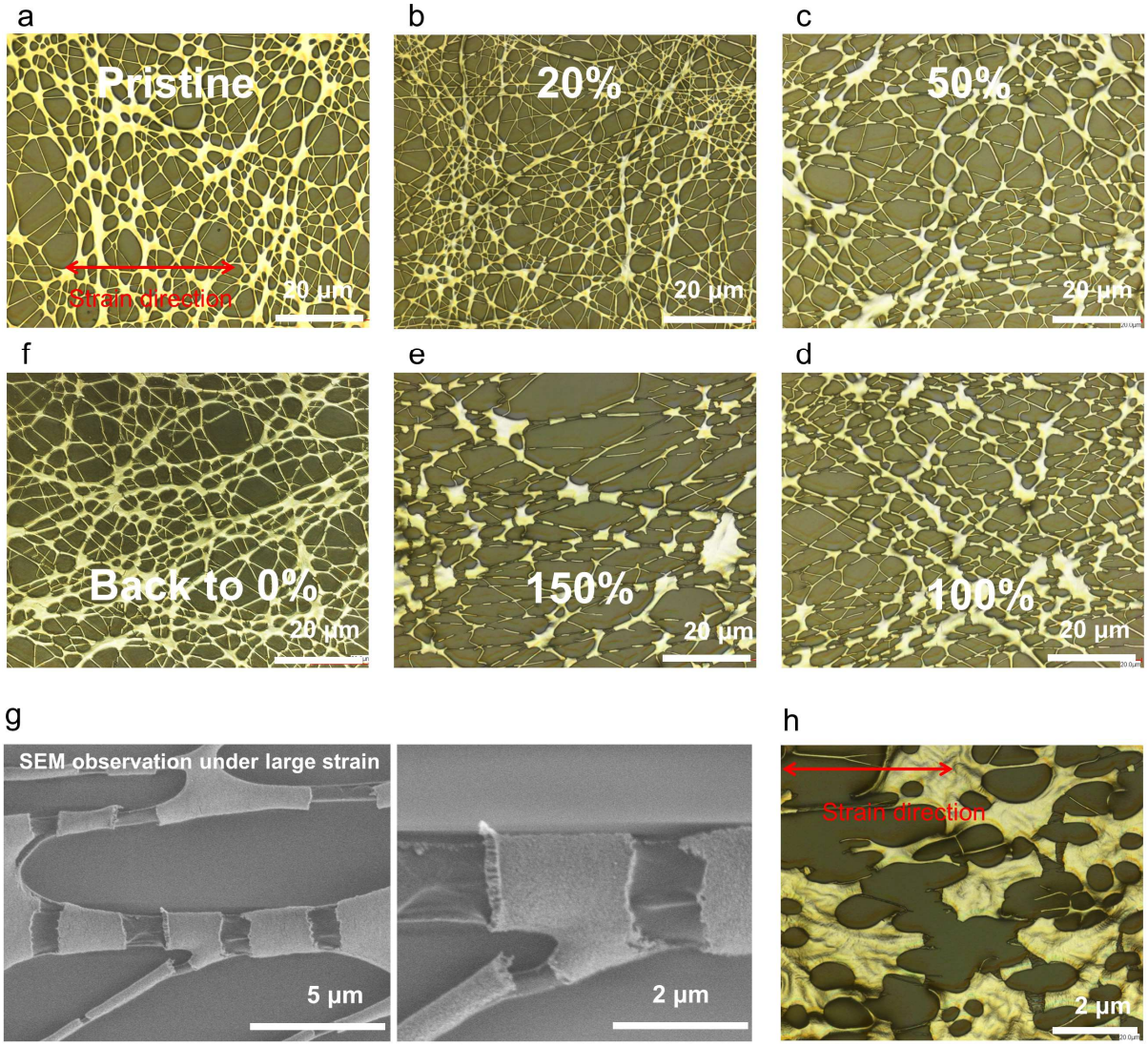

fig. S3. Surface morphology changes of PU–PDMS nanomesh sensors during strain. **a-f.** Surface morphology changes during strain from 0–20–50–100–150–0%. Continuous mesh structure maintains even at large strain of 150%. The "denser" parts or the clusters at 0% strain are attributed to the existence of larger PU–PDMS nanomesh bundles, mostly at junctions, these bundles will be elongated at larger strains. w/w of hexane/PDMS=1/160. **g.** SEM images of strained device under 130% strain. w/w of hexane/PDMS=1/160. **h.** SEM images of strained device under 70% strain. w/w of hexane/PDMS=1/40.

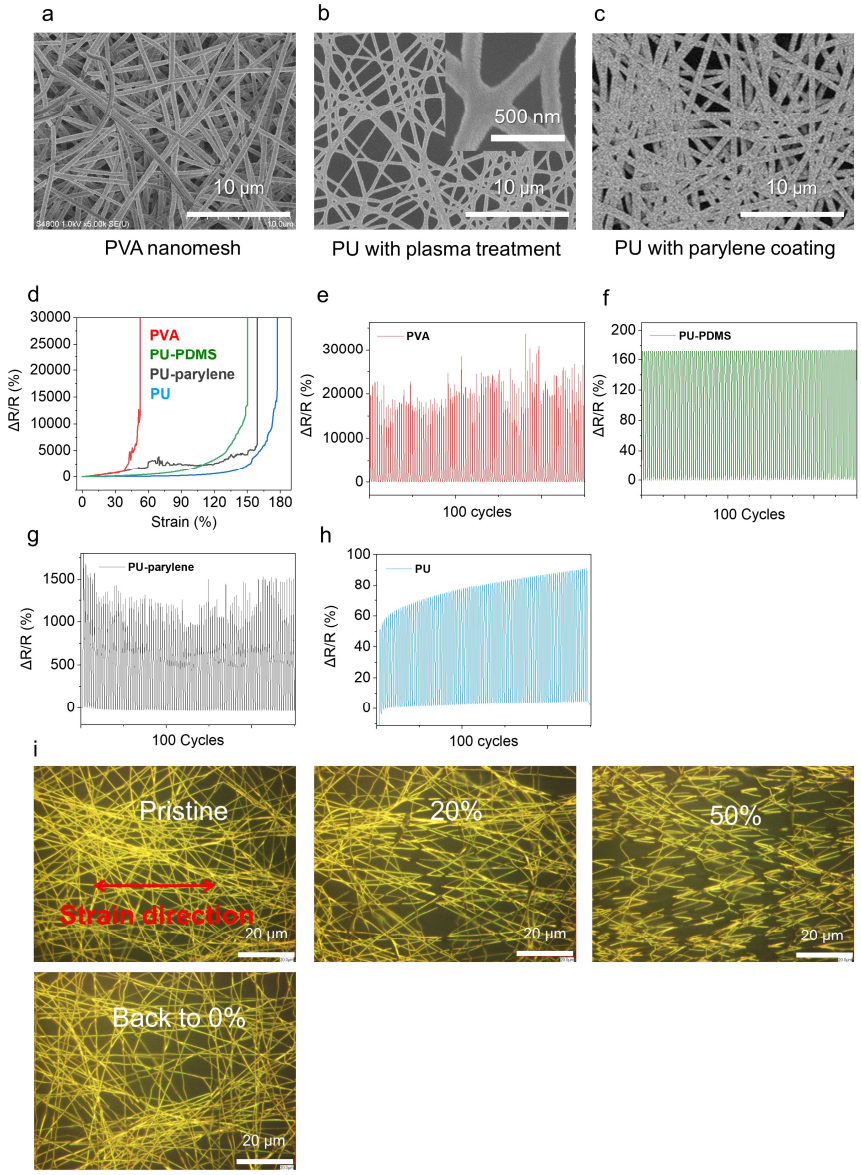

fig. S4. Characterization of three different nanomesh conductors and their comparison with PU–PDMS nanomesh sensor on electromechanical properties. The three nanomesh devices were made from PVA nanomesh, plasma treated PU nanomesh, and parylene coated PU nanomesh, respectively. **a-c**. SEM images of nanomesh conductors made of PVA nanomesh, plasma treated PU nanomesh, and parylene coated PU nanomesh, respectively. Inset SEM image evidences the connected junctions of plasma treated PU nanomeshes. **d**. Fail strain comparison of different nanomesh conductors. **e-h**. Cyclic test for the four different devices for 100 stretching/releasing cycles to 30% strain. w/w of hexane/PDMS=1/160. **i**. Surface morphology changes of bare PU nanomesh conductors during strain from 0–20–50–0% strain. Nanomesh breaks even at 20% strain, cracks become larger while increasing strain. All the breakages are permanent after releasing strain to 0%.

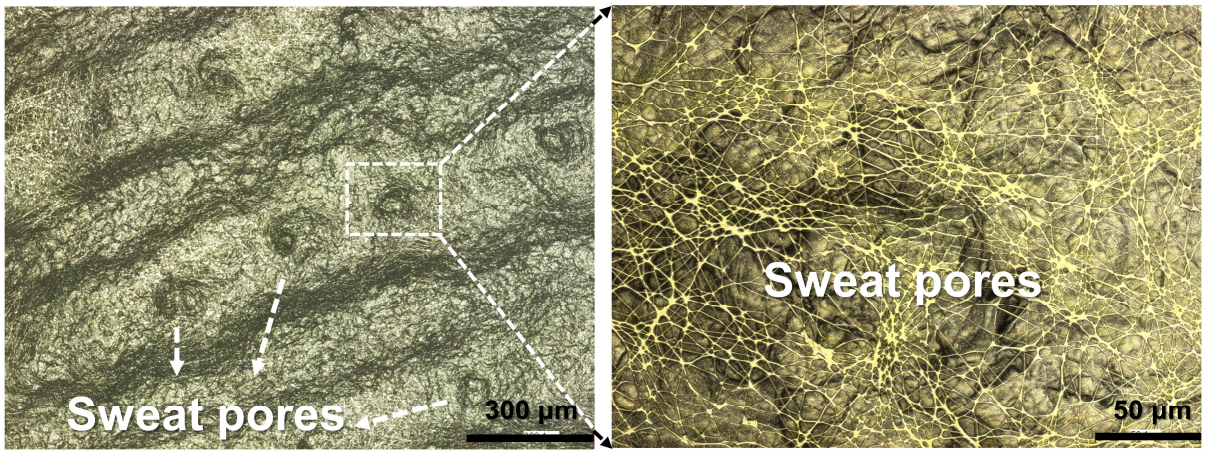

fig. S5. Microscopical images of the device on fingertip replica, demonstrating distinct sweat pore features. w/w of hexane/PDMS=1/160.

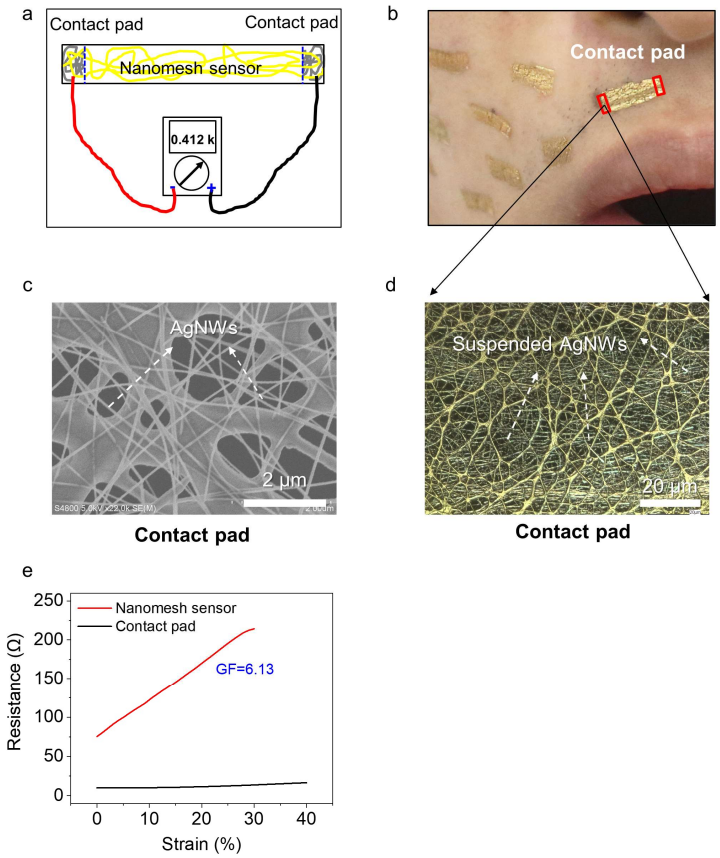

fig. S6. Resistance measurement design for speech facial strain mapping. **a**. Contact pads are at the two ends of PU–PDMS nanomesh sensor, which are fabricated by effective dip coating after nanomesh sensor fabrication. **b**. Enlarged photograph of nanomesh sensors on human face, red rectangles presents contact pads. **c**. SEM image of contact pad (AgNW nanomesh) showing distinct and abundant AgNWs attachment. **d**. Microscopic image of AgNW nanomesh. **e**. Electrical responses of nanomesh sensor and contact pad. Nanomesh sensor has linear resistance change in 0-30% strain, the strain range is sufficient enough for face strain detection during speech (<25% strain). The gauge factor of nanomesh sensor is calculated to be ~6.13. Contact pad exhibits strain insensitive stretchability up 40% strain, which is also more conductive than nanomesh sensor.

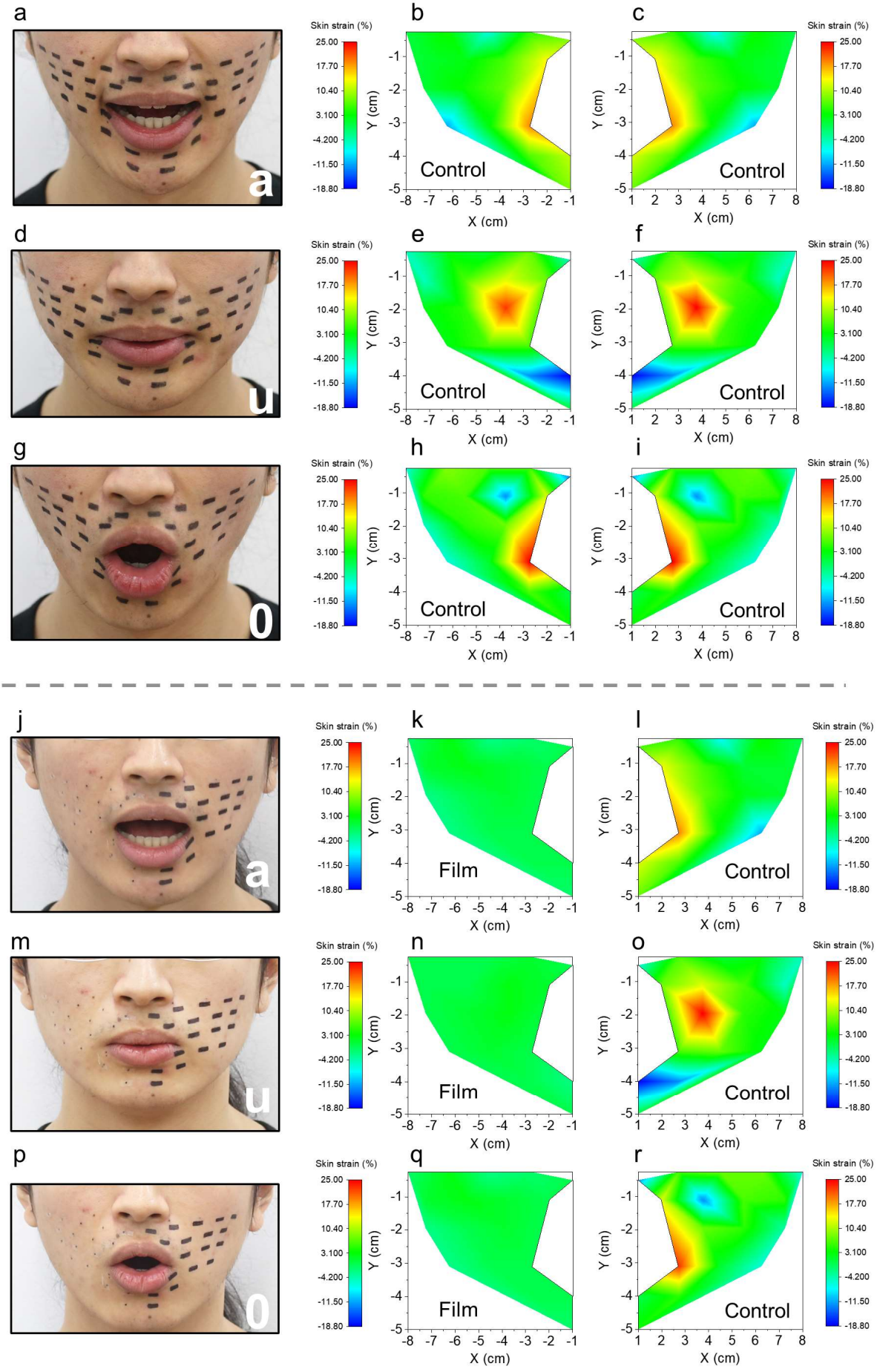
a
b
c
d
e
f
g
h
i
j
k
l
m
n
o
p
q
r
a
u
o
Control
Film
Skin strain (%)
25.00
17.70
10.40
3.100
-4.200
-11.50
-18.80
Y (cm)
X (cm)

fig. S7. Facial skin strain mapping during speech of ‘a’, ‘u’, and ‘o’ with black markers or PDMS films on the face. Strain results are derived from length measurement by a ruler. **a-i**. Facial skin strain mapping during speech of ‘a’, ‘u’, and ‘o’ using black marker on both the left and right sides of the face. **a**. Photograph of the face during speech of ‘a’. **b**. Strain mapping of the right side of the face during speech of ‘a’. **c**. Strain mapping of the left side of the face during speech of ‘a’. **d**. Photograph of the face during speech of ‘u’. **e**. Strain mapping of the right side of the face during speech of ‘u’. **f**. Strain mapping of the left side of the face during speech of ‘u’. **g**. Photograph of the face during speech of ‘o’. **h**. Strain mapping of the right side of the face during speech of ‘o’. **i**. Strain mapping of the left side of the face during speech of ‘o’. **j-r**. Facial skin strain mapping during speech of ‘a’, ‘u’ and ‘o’ with film-type PDMS films on the right side of the face and black markers on the left side of the face. **j**. Photograph of the face during speech of ‘a’. **k**. Strain mapping of the right side of the face during speech of ‘a’. **l**. Strain mapping of the left side of the face during speech of ‘a’. **m**. Photograph of the face during speech of ‘u’. **n**. Strain mapping of the right side of the face during speech of ‘u’. **o**. Strain mapping of the left side of the face during speech of ‘u’. **p**. Photograph of the face during speech of ‘o’. **q**. Strain mapping of the right side of the face during speech of ‘o’. **r**. Strain mapping of the left side of the face during speech of ‘o’.

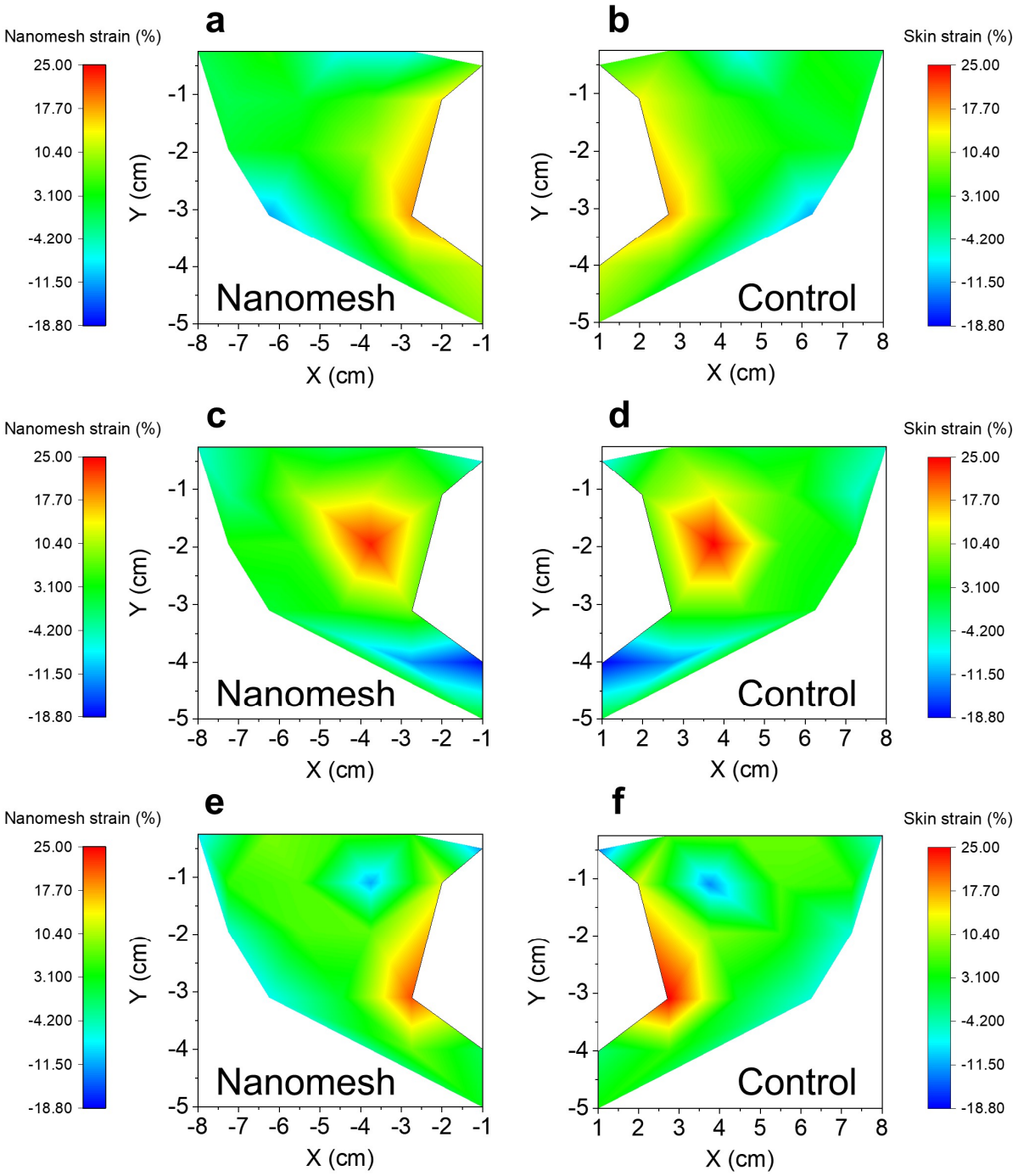

fig. S8. Facial skin strain mapping during speech of 'a', 'u', and 'o' with nanomesh sensor on the right side of the face and black markers on the left side of the face. Strain results are derived from length measurement by ruler. **a**. Strain mapping of the right side of the face during speech of 'a'. **b**. Strain mapping of the left side of the face during speech of 'a'. **c**. Strain mapping of the right side of the face during speech of 'u'. **d**. Strain mapping of the left side of the face during speech of 'u'. **e**. Strain mapping of the right side of the face during speech of 'o'. **f**. Strain mapping of the left side of the face during speech of 'o'.

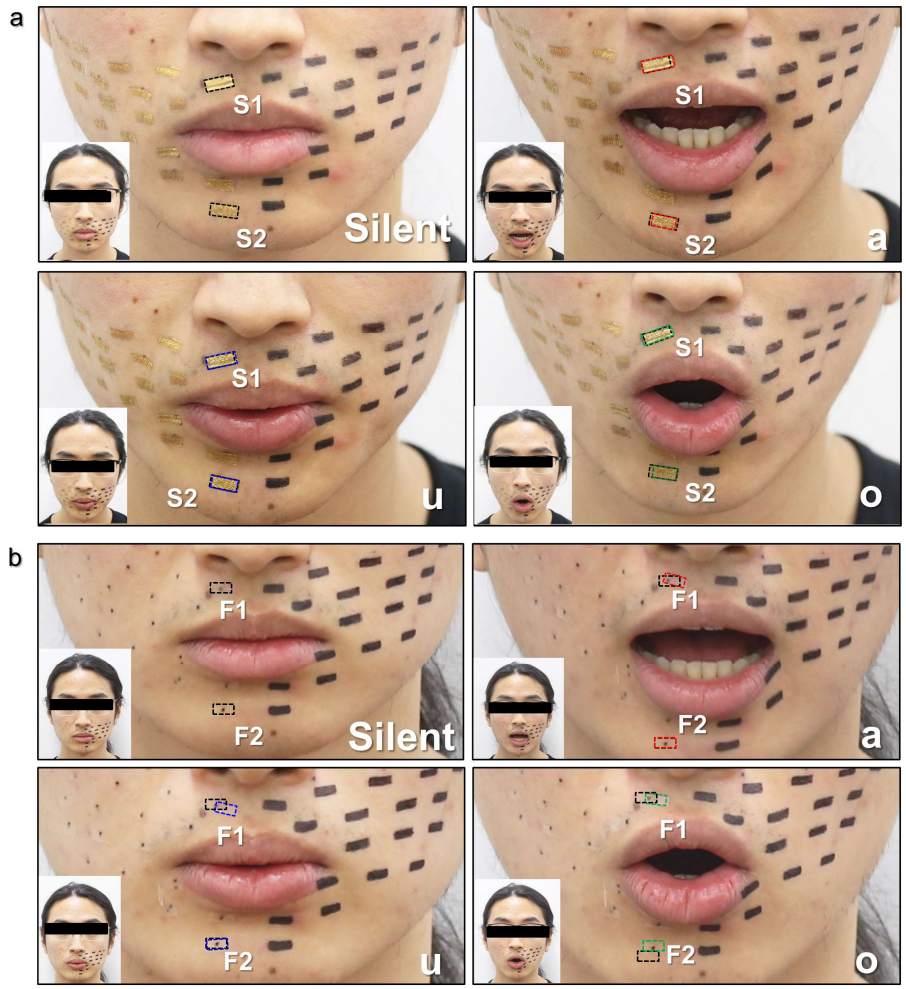

fig. S9. On-skin behaviour comparison between nanomesh sensors and film-type PDMS samples. **a.** Photographs showing subject wearing nanomesh sensors on the right side of the face and markers on the left side of the face in silent, 'a', 'u', and 'o' vocal states. Black, red, purple, and green rectangles represent shape and locations of two sensors (S1, S2) in four different states, respectively. The nanomesh sensors are well-maintained on the face during different speech. **b.** Photographs showing subject wearing PDMS thin films on the right side of the face and markers on the left side of the face in silent, 'a', 'u', and 'o' vocal states. Black, red, purple, and green rectangles represent shape and locations of two PDMS films (F1, F2) in four different states, respectively. The film will supress/constrain skin strain due to poor mechanical compliance. Film-type samples experience slippage and detachment while being strained or compressed, due to poor adhesion to human skin. Insets are photographs of the whole face.

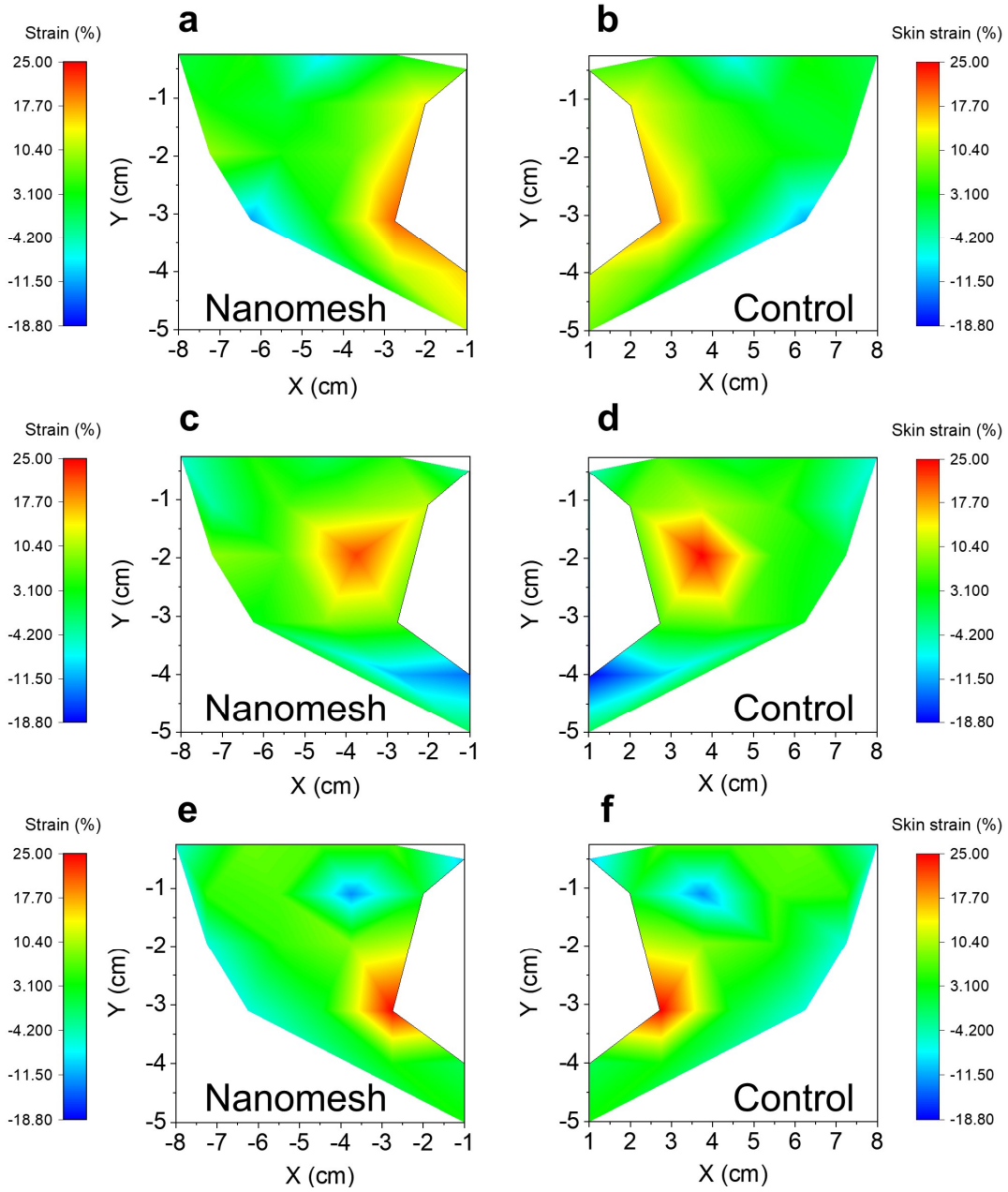

fig. S10. Facial skin strain mapping during speech of ‘a’, ‘u’ and ‘o’ with nanomesh sensors on the right side of the face and black markers on the left side of the face after 3.5 h wearing. Strain results on the left side of the face are derived from length measurement by a ruler; results on the right side of the face are derived from resistance and gauge factor. **a**. Strain mapping of the right side of the face during speech of ‘a’. **b**. Strain mapping of the left side of the face during speech of ‘a’. **c**. Strain mapping of the right side of the face during speech of ‘u’. **d**. Strain mapping of the left side of the face during speech of ‘u’. **e**. Strain mapping of the right side of the face during speech of ‘o’. **f**. Strain mapping of the left side of the face during speech of ‘o’.

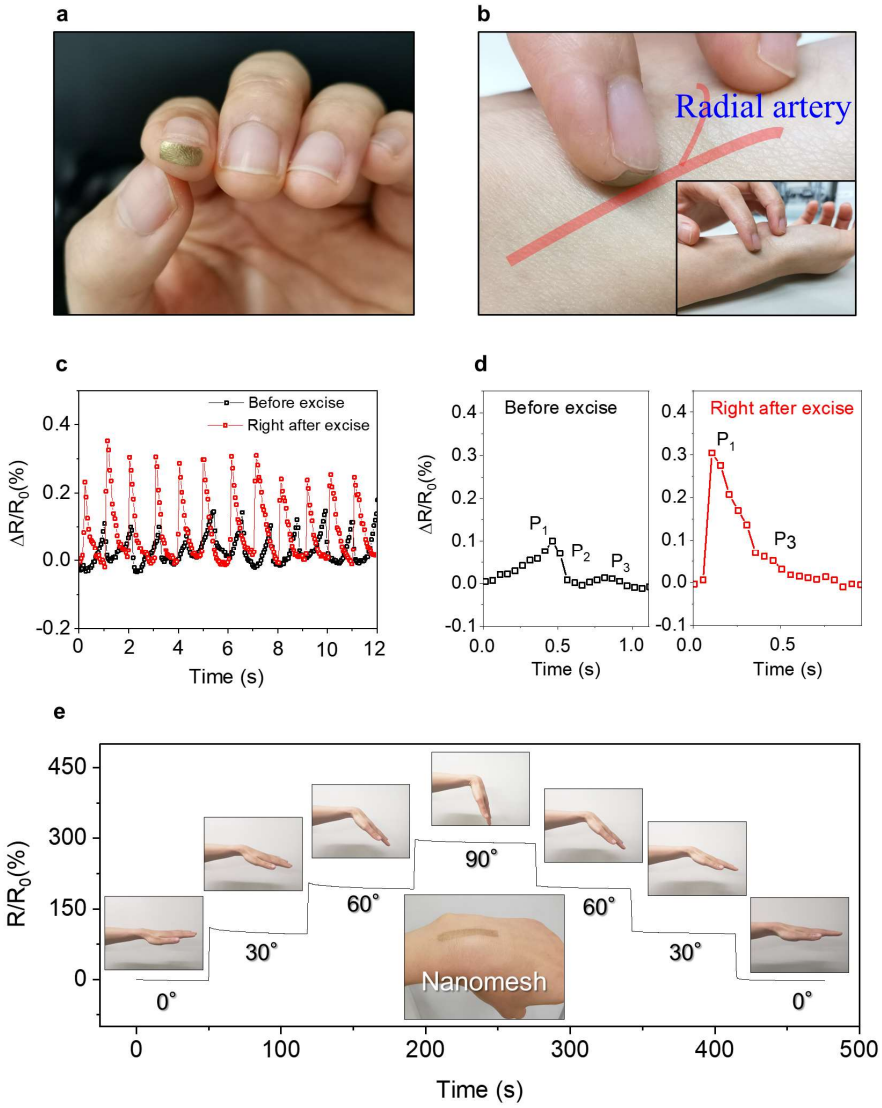

fig. S11. Nanomesh strain gauge for human wrist pulse and wrist bending detection. **a**. Photograph shows a fine device on human index fingertip, indicating excellent skin conformability. **b**. Photographs of picking up human wrist pulse signals, nanomesh device adheres to the free edge of index fingertip. **c**. Electrical responses obtained from two boy states: before excise and right after excise. **d**. Enlarged single pulse for electrical responses obtained from two body states: before excise and right after excise. PDMS/hexane w/w: 1/40. **e**. Accurate and stable wrist bending degree measurement. PDMS/hexane w/w: 1/160.

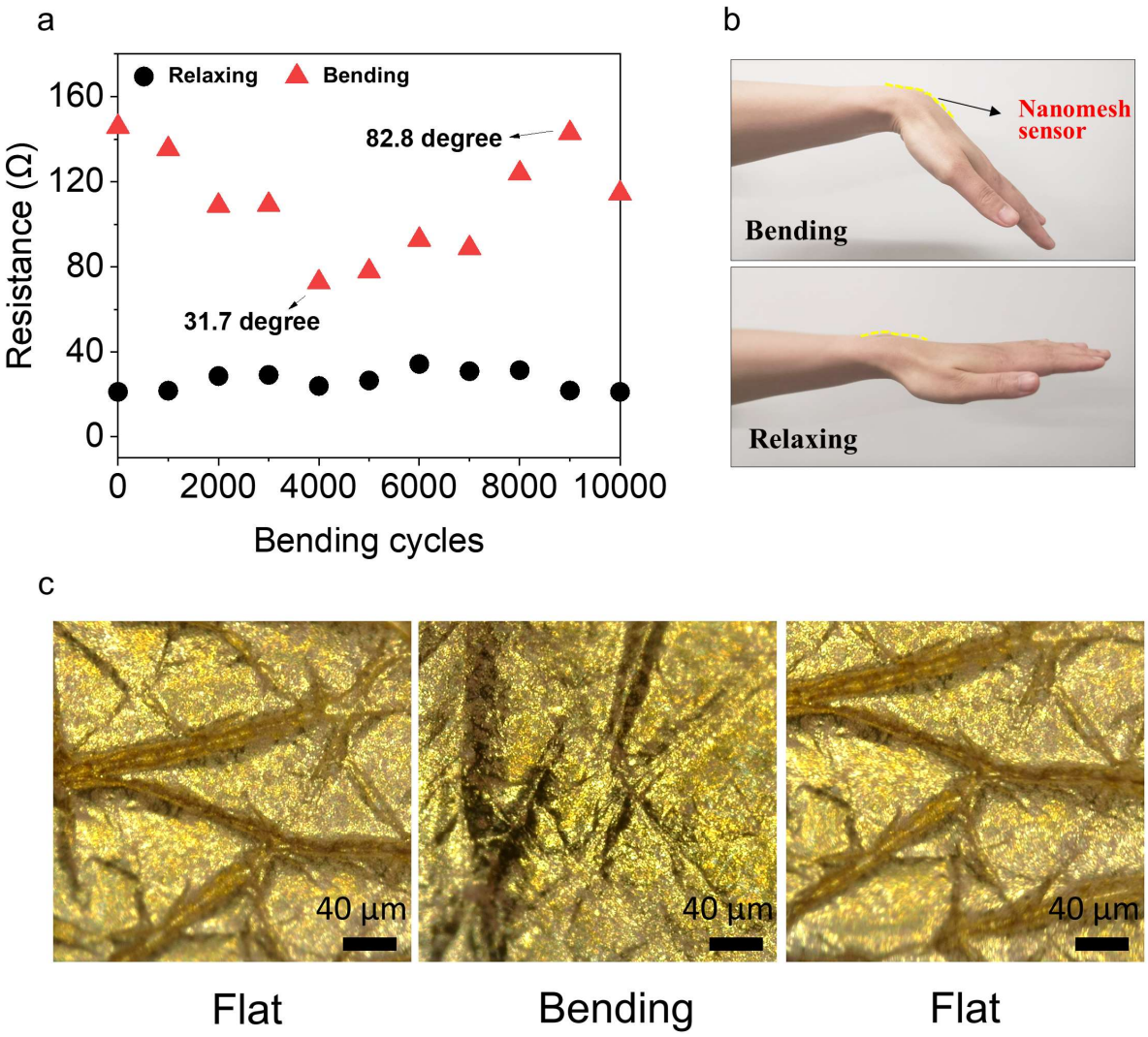

fig. S12. Durability test as strain gauge for wrist bending monitoring for 10,000 cycles. PDMS/hexane w/w: 1/160**. a.** Resistance change for 10,000 cycles wrist bending motions**. b.** Photos showing bending and flat states, respectively. **c.** Microscopical images of nanomesh sensor under different states after 10,000-cycle flexion test with mobile digital microscope, demonstrating the well-maintained structural integrity of nanomesh and device conformability with skin after long-term cyclic test.

Materials	Electrical property	Thickness (μm)	Weight (mg/cm²)	Gauge factor	Linearity	Structure	Durability		Applications	Ref
							Condition	Degradation ($R'-R_0)/R_0$)		
CNT-PDMS (AFM, 2012)	~ MΩ	320		4.9/29.1	5%	Film	50%, 100 cycles	500	Resistive strain gauge	40
Ag–Au NW/SBS (Nat. Nanotech, 2018)	30,000 S/cm	> 60				Film	30%, 3000 cycles	2	Heating element, stimulator and EMG electrodes	47
AuNWs/PDMS (Adv. Mat, 2019)	~ 200 Ω	> 100		10–1365	10%	Film	0%, 1000 cycles	0	Resistive strain gauge	48
Ag flake/polymer (ACS Nano, 2019)	3086 S/cm					Film	50%, 1000 cycles	0.3	Interconnect, EMG electrodes	49
Graphene (Adv. Func. Mat, 2015)	~10.5 Ω/□	550		15–29		Film	50%, 10000 cycles	0.65	Resistive strain gauge	13
Substrate-free nanomesh (Nat. Nanotech, 2017)	5.3 Ω/□	0.1	0.19			Mesh	25%, 500 cycles	0.23	Interconnect, EMG electrodes	42
AgNWs/PU (Small, 2019)	4 Ω/□	0.125				Mesh	Bending 360/m curvature, 500000 cycles	0.012	ECG electrodes	50
AgNWs/PU (Adv. Mat, 2019)	~0.37 Ω/□	< 3	1.92			Mesh	70%, 1000 cycles	0.82	Resistive sensor and EMG electrodes	41
Substrate-free Au nanomesh (Materials Today Physics, 2020)	40-60 Ω/□	0.03		0389/2.44	30%	Mesh	Bending, 3000 cycles	<1.5%	Resistive strain gauge	51
Au-PU/PDMS nanomesh (this work)	**0.82 Ω/□**	**0.43**	**0.12**	7.26-46.3	**60%**	**Mesh**	**60%, 5000 cycles**	**0.03**	**Resistive strain gauge**	
							12 h, 40% stretch holding	**Drift error: 0.053**		

table S1. Comparison with recently reported representative skin-mountable sensors on materials, gas permeability, thickness, conductivity, weight, stretchability, linearity, sensitivity, and durability. Light green shaded are breathable sensors. R′ is the resistance at 0% strain after cyclic test.